ELSEVIER

www.elsevier.nl/locate/jorganchem

Journal of Organometallic Chemistry 609 (2000) 89–94

Journal of Organometallic Chemistry

The clusters $HRu_3W(\eta^5\text{-Cp})(CO)_{11-x}(PPh_3)_xBH$ ($x = 1, 2$): preparations, characterizations and the crystal structure of $HRu_3W(\eta^5\text{-Cp})(CO)_{10}(PPh_3)BH$

Catherine E. Housecroft [a,*], Dorn M. Nixon [b], Arnold L. Rheingold [c]

[a] *Institut für Anorganische Chemie, Spitalstrasse 51, Basel CH-4056, Switzerland*
[b] *Department of Chemistry, University of Cambridge, Lensfield Road, Cambridge CB2 1EW, UK*
[c] *Department of Chemistry, University of Delaware, Newark, DE 19716, USA*

Received 19 February 2000; received in revised form 16 April 2000

Abstract

The clusters $HRu_3W(\eta^5\text{-Cp})(CO)_{11-x}(PPh_3)_xBH$ ($x = 1, 2$) have been prepared by reaction of PPh_3 with $HRu_3W(\eta^5\text{-Cp})(CO)_{11}BH$ after Me_3NO–MeCN-activation; $HRu_3W(\eta^5\text{-Cp})(CO)_{10}(PPh_3)BH$ has also been made by the reaction of $HRu_3(CO)_8(PPh_3)B_2H_5$ with $[(\eta^5\text{-Cp})W(CO)_3]_2$. The cluster-bound hydrogen atoms respond to the charge density changes as PPh_3 is introduced into $HRu_3W(\eta^5\text{-Cp})(CO)_{11}BH$, and proton chemical shift correlations are presented for this and related systems. The single crystal structure of $HRu_3W(\eta^5\text{-Cp})(CO)_{10}(PPh_3)BH$ has been determined.

Keywords: Ruthenium; Boron; Heterometallic cluster; Hydride; Phosphine

1. Introduction

Our interest in homometallic and heterometallic butterfly clusters containing an interstitial boron atom has been wide ranging [1–3] and has included studies of the reactivity of the boron centre and the use of these clusters as building blocks to higher nuclearity clusters in which the boron atom becomes fully interstitial. We have reported a number of heterometallic butterfly species containing an $Ru_3M'B$-core in which $M' = Mo$ [4], W [4], Fe [5], Rh [6], Ir [6]. In particular, we have pointed to the fact that changing the metal can lead to a change in the number of cluster-bound hydrogen atoms (as a response to a change in metal electron count) and that this, in turn, can provide a means of controlling the chemistry of the cluster, for example in the assembly of linked clusters [7]. In this paper, we look at methods of introducing a PPh_3 ligand into $HRu_3W(\eta^5\text{-Cp})(CO)_{11}BH$, both by PPh_3-for-CO substitution and by cluster expansion starting with the PPh_3 ligand in an Ru_3-precursor. We compare the cluster hydrogen distributions in a series of isoelectronic heterometallic clusters in which the heterometal is varied, and correlate the ^{1}H-NMR spectroscopic chemical shifts of the cluster-bound hydrogen atoms to substitution pattern.

2. Experimental

2.1. General data

FT-NMR spectra were recorded on a Bruker WM 250 spectrometer (^{1}H) or AM 400 spectrometer (^{31}P, ^{11}B and ^{1}H); ^{1}H shifts are reported with respect to δ 0 for Me_4Si, ^{11}B-NMR with respect to δ 0 for $F_3B{\cdot}OEt_2$, and ^{31}P-NMR with respect to δ 0 for 85% H_3PO_4. Solution infrared spectra were recorded on a Perkin–Elmer FT 1710 spectrophotometer, and fast atom bombardment (FAB) mass spectra using Kratos instruments (3-NBA matrix = 3-nitrobenzyl alcohol).

* Corresponding author. Tel.: +41-61-2671004; fax: +41-61-2671014.
E-mail address: catherine.housecroft@unibas.ch (C.E. Housecroft).

0022-328X/00/$ - see front matter
PII: S0022-328X(00)00216-3

Reactions were carried out under argon using standard Schlenk techniques; solvents were pre-dried and distilled under N_2. Separation of products was by thin layer plate chromatography (TLC) using Kieselgel 60-PF-254 (Merck). Photolysis experiments used a mercury high-pressure lamp with the sample contained in a quartz tube flushed with argon. $HRu_3W(\eta^5\text{-}Cp)(CO)_{11}BH$ (**1**) [4] and $HRu_3(CO)_8(PPh_3)B_2H_5$ [8] were prepared as previously reported. Triphenylphosphine was used as supplied (Aldrich). Yields are quoted with respect to starting cluster; yields are often variable and typical values are quoted. Abbreviations: Cp, C_5H_5; Cp*, C_5Me_5.

2.2. Photolysis of $HRu_3W(\eta^5\text{-}Cp)(CO)_{11}BH$ with PPh_3

$HRu_3W(\eta^5\text{-}Cp)(CO)_{11}BH$ (11 mg, 0.013 mmol) and PPh_3 (3 mg, 0.013 mmol) were dissolved in THF (1 ml) and photolysed for 21 h during which time, the orange solution darkened. After TLC separation eluting with hexane–CH_2Cl_2 (2:1), the following fractions were collected and identified by comparison with their literature spectroscopic data: $H_4Ru_4(CO)_{12}$ (trace amounts) [9], $H_4Ru_4(CO)_{11}(PPh_3)$ ($\approx 10\%$) [10], unreacted $HRu_3W(\eta^5\text{-}Cp)(CO)_{11}BH$ ($\approx 40\%$) and $H_3Ru_3W(\eta^5\text{-}Cp)(CO)_{11}$ ($\approx 40\%$) [4].

2.3. Photolysis of $HRu_3(CO)_8(PPh_3)B_2H_5$ with $[(\eta^5\text{-}Cp)W(CO)_3]_2$

$HRu_3(CO)_8(PPh_3)B_2H_5$ (8 mg, 0.001 mmol) was dissolved in THF (0.5 ml) and added to $[(\eta^5\text{-}Cp)W(CO)_3]_2$ (7 mg, 0.001 mmol). The resulting solution was photolysed for 8 h. TLC separation, eluting with hexane–CH_2Cl_2 (2:1) gave a number of fractions, but only the three main fractions were collected. The first fraction was identified as $Ru_3(CO)_{12}$ ($\approx 20\%$); the second band was $H_4Ru_4(CO)_{11}(PPh_3)$ ($\approx 10\%$) [10]. The third fraction (orange, $\leq 10\%$) was $HRu_3W(\eta^5\text{-}Cp)(CO)_{10}(PPh_3)BH$ (**2**). The low yield meant that only partial characterization (^{11}B-NMR, IR spectroscopic data and FABMS) was possible; full data are given in Section 2.4.

2.4. Activation of $HRu_3W(\eta^5\text{-}Cp)(CO)_{11}BH$ with Me_3NO–MeCN and reaction with PPh_3

$HRu_3W(\eta^5\text{-}Cp)(CO)_{11}BH$ (14 mg, 0.016 mmol) was dissolved in CH_2Cl_2 (6 ml) and MeCN (2 ml). The solution was cooled to -76°C in a dry ice–acetone bath and a molar equivalent of Me_3NO (1.2 mg) dissolved in MeCN (5 ml) was added dropwise. The reaction was monitored by IR spectroscopy (new absorptions appeared at 2068, 2041, 2011, 1991 and 1952 cm^{-1}) and when no more $HRu_3W(\eta^5\text{-}Cp)(CO)_{11}BH$ was evident (after 15 min), the solution was filtered into a flask containing PPh_3 (4 mg, 0.016 mmol). After 90 min stirring, solvent was removed in vacuo. The products were separated by TLC eluting with hexane–CH_2Cl_2 (3:1). The first fraction was $HRu_3W(\eta^5\text{-}Cp)(CO)_{11}BH$ (orange, $\approx 20\%$). The main product was $HRu_3W(\eta^5\text{-}Cp)(CO)_{10}(PPh_3)BH$ (**2**), (orange, typically $\approx 50\%$) and the final band was $HRu_3W(\eta^5\text{-}Cp)(CO)_9(PPh_3)_2BH$ (**3**), ($\approx 10\%$). Smaller fractions were observed on the TLC plate but were not collected. Compound **2**: ^{1}H-NMR ($CDCl_3$, 298 K) δ +7.5–7.4 (m, Ph), +5.21 (s, $\eta^5\text{-}C_5H_5$), −5.6 (br, Ru–H–B), −20.4 (d, J(PH) 2.3 Hz, Ru–H–Ru); ^{11}B-NMR ($CDCl_3$, 298 K) δ +129; ^{31}P-NMR ($CDCl_3$, 298 K) δ +37.5; IR (hexane, cm^{-1}) ν(CO) 2082 w, 2067 m, 2045 vs, 2013 s, 2000 s, 1989 m, 1979 m, 1958 m, 1902 m. FABMS: 1106 (P^+, correct isotope distribution) with ten sequential CO losses; calc. for $^{12}C_{33}$ $^1H_{22}$ ^{11}B $^{16}O_{10}$ ^{31}P $^{101}Ru_3$ ^{184}W; 1107.

2.4.1. Compound **3**

^{1}H-NMR ($CDCl_3$, 298 K) δ +7.6–7.4 (m, Ph), +5.36 (s, $\eta^5\text{-}C_5H_5$), −5.6 (br, Ru–H–B), −19.5 (d, J(PH) 8.5 Hz, Ru–H–Ru); ^{11}B-NMR ($CDCl_3$, 298 K) δ +129; IR (hexane, cm^{-1}) ν(CO) 2067 w, 2057 m, 2046 m, 2025 m, 2011 s, 1993 m, 1978 m, 1965 m, 1955 w, 1948 w, 1936 w, 1885 m. FABMS: 1342 (P^+, correct isotope distribution) with nine sequential CO losses; calc. for $^{12}C_{50}$ $^1H_{37}$ ^{11}B $^{16}O_9$ $^{31}P_2$ $^{101}Ru_3$ ^{184}W; 1341.

2.5. Crystal structure determination of **2**

A suitable crystal of **2** was grown from a CH_2Cl_2 solution kept at 0°C for several days. Crystallographic data are collected in Table 1. All specimens screened diffracted weakly and broadly indicative of high thermal activity. Systematic absences in the diffraction data allowed the unique assignment of the orthorhombic space group shown. The unit-cell dimensions were obtained from the angular settings of 25 reflections ($20 < 2\theta < 30$). Data were collected to a $2\theta_{max} = 45°$ yielding 1773 observed reflections. The structure was solved by direct methods and refined by full-matrix, least-squares methods. The metal, phosphorus and oxygen atoms were refined anisotropically. Several of the carbon atoms became non-positive-definite on attempted anisotropic refinement and the effort was abandoned. Hydrogen atoms were placed in idealized locations. All software was included in the SHELXTL 5.0 library [11].

3. Results and discussion

The homometallic boride cluster $HRu_4(CO)_{12}BH_2$ undergoes phosphine substitution reactions relatively readily, with the first and second substitution positions for mondentate ligands such as PPh_3 being at remote

wingtip Ru atoms and in equatorial sites. For the disubstituted compound $HRu_4(CO)_{10}(PPh_3)_2BH_2$, two isomers are formed with substitution patterns (1,10) and (1,11) using the numbering scheme in Scheme 1 [12]. In the case of the incoming ligand being Ph_2PH, the first site of attack is an equatorial, wingtip Ru site (e.g. site 1 in Scheme 1), with the second substitution occurring at an equatorial, hinge Ru atom to give a mixture of isomers, with substitution patterns (1,6) and either (1,8) or (1,9) [13]. We initially undertook the study of phosphine substitution in the heterometallic compound $HRu_3W(\eta^5\text{-Cp})(CO)_{11}BH$ (**1**), (Scheme 1), as a comparative investigation with respect to substitution in $HRu_4(CO)_{12}BH_2$. In **1**, one wingtip site is occupied by a $W(\eta^5\text{-Cp})(CO)_2$ unit, and, compared to $HRu_4(CO)_{12}BH_2$ (**1**) has one fewer cluster hydrogen atoms.

Table 1
Crystallographic data for compound **2**

Formula	$C_{33}H_{22}BO_{10}PRu_3W$
F_w	1107.35
Crystal size (mm)	$0.21 \times 0.21 \times 0.23$
Crystal colour and habit	Orange cube
Crystal system	Orthorhombic
Space group	*Pbca*
Unit cell dimensions	
a (Å)	19.539(4)
b (Å)	10.727(2)
c (Å)	33.076(7)
V (Å^3)	6933(2)
Z	8
D_{calc} (g cm^{-3})	2.122
Radiation	Mo–K_α ($\lambda = 0.71073$ Å)
Temperature (K)	293(2)
Diffractometer	Bruker P4
2θ range (°)	2.08–22.49
Independent reflections (observed [$4\sigma(F_o)$])	4512, 1893
$R(F)$, $R(wF^2)$ (%)	8.99, 17.45
Goodness-of-fit	1.107
Data:parameter ratio	16.8
Largest difference peak and hole (e Å^{-3})	1.76 and −1.99

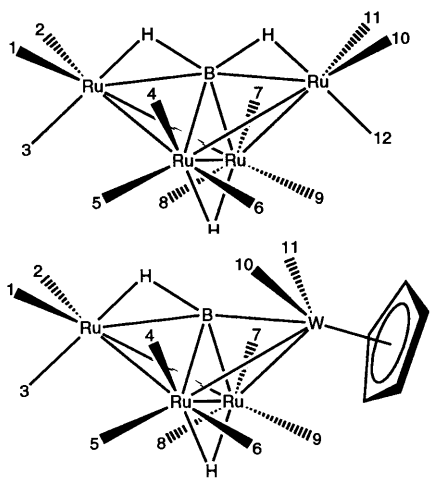

Scheme 1.

Initial attempts at direct reaction between **1** and PPh_3 under ambient conditions (stirring in CH_2Cl_2 solution at room temperature (r.t.) for 4 days) were unsuccessful, giving back only starting material. Since these conditions failed to produce a substituted derivative of **1**, we attempted use of photolysis; reaction did occur after an overnight photolysis. In addition to unreacted starting cluster, the main products were the non-boron containing tetrahedral clusters $H_4Ru_4(CO)_{11}(PPh_3)$ and $H_3Ru_3W(\eta^5\text{-Cp})(CO)_{11}$. It seems likely that the latter compound (which, in solution, exists as two isomers [4]) was formed by boron abstraction by the PPh_3 Lewis base and closure of the Ru_3W framework from a 62-electron butterfly to a 60-electron tetrahedron (Scheme 2). This result in itself is interesting since competitive reactions of this nature had not proved a problem in photolysis reactions of $HRu_4(CO)_{12}BH_2$ with PPh_3 or other phosphines [12]. The cluster closure in Scheme 2 requires not only cluster-hydrogen atom redistribution, but also the gain of a hydrogen atom during boron abstraction. That the reaction is not simple is supported by the formation of $H_4Ru_4(CO)_{11}(PPh_3)$.

The original synthesis of $HRu_3W(\eta^5\text{-Cp})(CO)_{11}BH$ [4] proceeded by the reaction of $HRu_3(CO)_9BH_4$ or $HRu_3(CO)_9B_2H_5$ with $[(\eta^5\text{-Cp})W(CO)_3]_2$. Since the preparation of $HRu_3(CO)_8(PPh_3)B_2H_5$ is facile [8], we decided to use a parallel strategy to attempt to prepare $HRu_3W(\eta^5\text{-Cp})(CO)_{10}(PPh_3)BH$. Photolysis of a THF solution of $HRu_3(CO)_8(PPh_3)B_2H_5$ and $[(\eta^5\text{-Cp})W(CO)_3]_2$ resulted in the formation of $HRu_3W(\eta^5\text{-Cp})(CO)_{10}(PPh_3)BH$ (**2**), in low yield. Evidence for its formation came from the appearance in the FABMS of a parent ion with correct isotopomer distribution at $m/z = 1106$ with loss of ten CO ligands. In the ^{11}B-NMR spectrum of the product, a broad signal at δ +129 was indicative of the boron atom residing in a butterfly-shaped tetrametal core; the corresponding resonance for **1** is δ +132. Attempts to improve the yield of **2** via this reaction route, however, were unsuccessful.

The most fruitful approach to the synthesis of compound **2** was to activate compound **1** with respect to ligand substitution by using the well-tested methodology of CO replacement by the labile ligand MeCN. The reaction of **1** with Me_3NO and MeCN was monitored by using IR spectroscopy, and when absorptions due to **1** had been virtually fully replaced by those of a new compound (assumed to be an MeCN derivative), the reaction mixture was added to PPh_3. The reaction was monitored by IR spectroscopy, and was judged to be complete after 1.5 h. The major product of this reaction was $HRu_3W(\eta^5\text{-Cp})(CO)_{10}(PPh_3)BH$ (**2**); the reaction was reproducible although yields were rather varied,

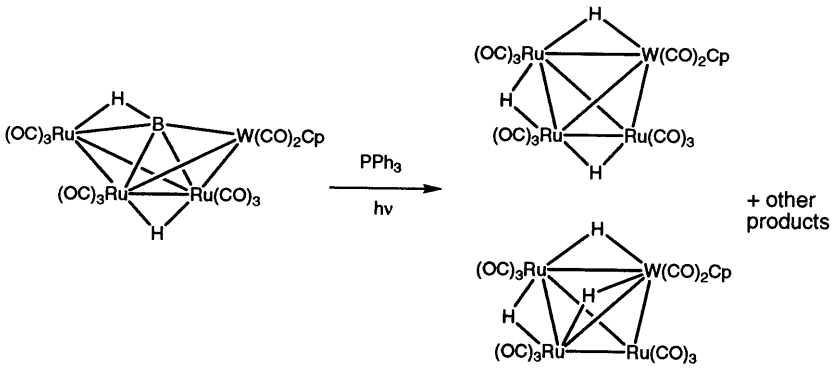

Scheme 2.

but typically about 50%. Some starting cluster **1** was always obtained back, as well as low yields of the disubstituted cluster $HRu_3W(\eta^5\text{-Cp})(CO)_9(PPh_3)_2BH$ (**3**). The FAB mass spectrum and ^{11}B-NMR spectrum of **2** obtained by this route were consistent with those recorded for the product of the reaction of $HRu_3(CO)_8(PPh_3)B_2H_5$ and $[(\eta^5\text{-Cp})W(CO)_3]_2$ (see above). The ^{31}P-NMR spectrum of **2** exhibited a single peak at δ +37.5; absence of any satellite peaks indicated that the phosphine ligand was bound to Ru rather than W. The ^{1}H-NMR spectrum was particularly diagnostic. A signal at δ −20.4 was characteristic of a hydride bridging two hinge Ru atoms. That this signal was a doublet with $J = 2.3$ Hz indicated long range ^{31}P–^{1}H coupling and was of a magnitude consistent with our previous observations in $HRu_4(CO)_{12-x}(PPh_3)_xBH_2$ ($x = 1$ or 2) for coupling between a wingtip bound PR_3 ligand and the hinge hydride. Further, the signal due to the Ru–H–B bridging hydrogen was observed at δ −5.6, and was significantly shifted with respect to that in the parent compound **1** (δ −6.6). We return to this diagnostic shift in signal later. Confirmation of the substitution position came from a single crystal structure determination of **2**.

Suitable crystals of **2** were grown from a cooled solution of **2** in CH_2Cl_2. Fig. 1 shows the molecular structure of **2**, and selected bond distances and angles are given in Table 2. The retention of the Ru_3W butterfly framework on going from **1** (which has also been structurally characterized [4]) to **2** was confirmed, as was the retention of the $W(CO)_2(\eta^5\text{-Cp})$ fragment in a wingtip site. As in **1**, the two W-attached CO ligand lean over towards the B atom, the latter being in a semi-interstitial position with respect to the metal core. The B atom lies 0.26 Å above the Ru(wingtip)–W(wingtip) axis. All CO ligands are terminally attached and bond parameters are unexceptional. The PPh_3 ligand occupies an equatorial wingtip site on atom Ru(3), and this site preference matches that in $HRu_4(CO)_{11}(PPh_3)BH_2$ [12]. It is also consistent with the small J(PH) coupling constant observed for the Ru(hinge)–H–Ru(hinge) hydride (see above).

As mentioned earlier, the site of second substitution on going from $HRu_4(CO)_{11}(PPh_3)BH_2$ to $HRu_4(CO)_{10}(PPh_3)_2BH_2$ is the second wingtip Ru atom for the case of $L = PPh_3$, but a hinge Ru atom for $L = Ph_2PH$. For this boron-containing cluster, other hinge substitution has only been observed in the case of a didentate ligand with short backbone, for example, bis(diphenylphosphino)ethane in which a Ru(wingtip)–Ru(hinge) bridging mode is adopted. The disubstituted derivative $HRu_3W(\eta^5\text{-Cp})(CO)_9(PPh_3)_2BH$ (**3**), was only isolated in low yield. The FAB mass spectrum exhibited a parent ion (with an isotopic distribution matching that simulated) at 1342. In the ^{11}B-NMR spectrum, a signal at δ +129 indicated that the boron environment had not been perturbed on going from **2** to **3**. No well resolved ^{31}P-NMR spectrum could be obtained, but signals in the ^{1}H-NMR spectrum were diagnostic. A broad signal at δ −5.6 was assigned to the Ru–H–B hydrogen atom, and by comparison with the corresponding signals in compounds **1** and **2**, we could conclude that a $\{(CO)_2(PPh_3)$-

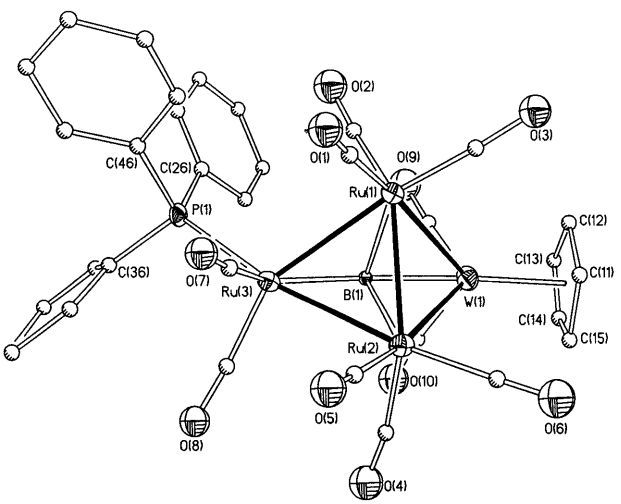

Fig. 1. Molecular structure of $HRu_3W(\eta^5\text{-Cp})(CO)_{10}(PPh_3)BH$ (**2**). Cluster hydrogen atoms were not located; phenyl and Cp–H atoms are omitted.

Table 2
Selected bond lengths (Å) and angles (°) in **2**

Bond distances			
W(1)–Ru(1)	2.986(3)	W(1)–Ru(2)	2.981(3)
W(1)–B(1)	2.12(3)	Ru(1)–Ru(2)	2.834(3)
Ru(1)–Ru(3)	2.899(4)	Ru(1)–B(1)	2.18(3)
Ru(2)–Ru(3)	2.857(4)	Ru(2)–B(1)	2.23(3)
Ru(3)–P(1)	2.357(9)	Ru(3)–B(1)	2.12(3)
Bond angles			
Ru(1)–W(1)–Ru(2)	56.71(7)	Ru(1)–W(1)–B(1)	46.9(8)
Ru(2)–W(1)–B(1)	48.3(8)	W(1)–Ru(1)–Ru(2)	61.56(9)
W(1)–Ru(1)–Ru(3)	91.24(10)	Ru(2)–Ru(1)–Ru(3)	59.77(10)
W(1)–Ru(1)–B(1)	45.1(7)	Ru(2)–Ru(1)–B(1)	50.8(8)
Ru(3)–Ru(1)–B(1)	46.6(7)	W(1)–Ru(2)–Ru(1)	61.73(9)
W(1)–Ru(2)–Ru(3)	92.16(10)	Ru(1)–Ru(2)–Ru(3)	61.24(11)
W(1)–Ru(2)–B(1)	45.1(7)	Ru(1)–Ru(2)–B(1)	49.3(8)
Ru(3)–Ru(2)–B(1)	47.2(7)	Ru(1)–Ru(3)–Ru(2)	58.99(8)
Ru(1)–Ru(3)–P(1)	110.6(2)	Ru(2)–Ru(3)–P(1)	167.8(2)
Ru(1)–Ru(3)–B(1)	48.6(8)	Ru(2)–Ru(3)–B(1)	50.6(8)
P(1)–Ru(3)–B(1)	118.4(8)	Ru(3)–B(1)–W(1)	167.6(14)
Ru(3)–B(1)–Ru(1)	84.8(10)	W(1)–B(1)–Ru(1)	88.0(10)
Ru(3)–B(1)–Ru(2)	82.2(10)	W(1)–B(1)–Ru(2)	86.6(10)
Ru(1)–B(1)–Ru(2)	80.0(8)		

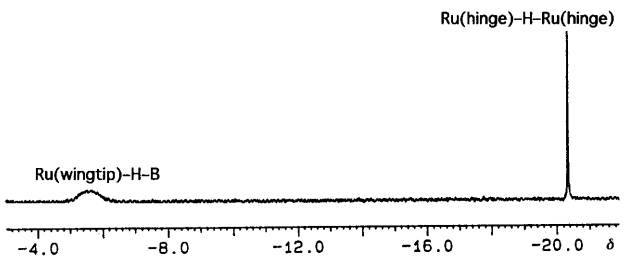

Fig. 2. Part of the ^{1}H-NMR spectrum (400 MHz, $CDCl_3$, 298 K) of compound **2** showing the signals due to the cluster-bound H atoms.

Ru–H–B} connectivity pattern was present for the wingtip Ru atom. A doublet in the ^{1}H-NMR spectrum at δ −19.5 showed a coupling of 8.5 Hz typical of *cis*-PH coupling and, therefore, indicated that the second PPh_3 ligand coordinates to a hinge Ru atom, *cis* to the Ru–H–Ru hydrogen atom. This signal would be expected to be a doublet of doublets, but no coupling between the Ru(wingtip)–P atom and the hydride could be resolved. In the related compound $HRu_4(CO)_{10}(Ph_2PH)_2BH_2$, the hinge hydride also appeared as a doublet ($J = 11.5$ Hz) and, moreover, in $HRu_4(CO)_{11}(Ph_2PH)BH_2$, no coupling between the Ru(wingtip)–P atom and the hydride could be resolved [13]. Using the numbering scheme in Scheme 1 for structure **1**, we therefore propose a substitution pattern in $HRu_3W(\eta^5\text{-Cp})(CO)_9(PPh_3)_2BH$ of (1,6), (1,9), (1,5) or (1,8); of these the (1,5) distribution would seem to be unlikely on steric grounds.

When assigning sites of PR_3 substitution in a cluster, the presence of hydrides is particularly useful in terms of using ^{1}H-NMR spectroscopy and observed values of J(PH) to aid the assignment of sites of substitution. One of the problems with boron-attached hydrogen atoms is that they give rise to broad signals in the ^{1}H-NMR spectrum (Fig. 2); in the absence of $^1H\{^{11}B\}$ decoupling experiments, it is not possible to resolve ^{31}P–^{1}H coupling in such signals. We have now prepared a series of phosphine substituted homo- and heterometallic boride clusters containing M_4 butterfly cores hosting a semi-interstitial boron atom, and have crystallographic data on representative members of the series which provide firm evidence for the location of the PR_3 substituents. Inspection of the data in Table 3 shows clearly that the chemical shift of the Ru(wingtip)–H–B hydrogen atom is sensitive to the presence of a Ru(wingtip) PR_3 substituent attached to the same Ru atom, while the shift of the signal due to the Ru(hinge)–H–Ru(hinge) hydride only responds to substitution at one of the Ru(hinge) atoms. While these results are not surprising in terms of the change in electron density at the Ru centre that must accompany PR_3-for-CO substitution, Table 3 brings together a

Table 3
^{1}H-NMR spectroscopic data for cluster-bound H atoms in a series of phosphine substituted M_4B-butterfly clusters

Compound	Site of substitution	δ Ru(wingtip)–H–B	δ Ru(hinge)–H–Ru(hinge) and (J(PH), Hz)	Ref.
$HRu_4(CO)_{12}BH_2$		−8.4 (2H)	−21.2	[14,15]
$HRu_4(CO)_{11}(PPh_3)BH_2$	Ru(wingtip)	−7.5; −8.6	−21.1 (2)	[12]
$HRu_4(CO)_{10}(PPh_3)_2BH_2$	2Ru(wingtip)	−7.5 (2H)	−21.1 (2.4)	[12]
$HRu_4(CO)_{11}(PPh_2H)BH_2$	Ru(wingtip)	−7.9; −8.5	−21.1 [a]	[13]
$HRu_4(CO)_{10}(PPh_2H)_2BH_2$	Ru(wingtip); Ru(hinge)	−8.0; −8.5	−20.4 [a] (11.5)	[13]
$HRu_3W(\eta^5\text{-Cp})(CO)_{11}BH$		−6.6	−20.4	[4]
$HRu_3W(\eta^5\text{-Cp})(CO)_{10}(PPh_3)BH$	Ru(wingtip)	−5.6	−20.4 (2.3)	This work
$HRu_3W(\eta^5\text{-Cp})(CO)_9(PPh_3)_2BH$	Ru(wingtip); Ru(hinge)	−5.6	−19.5 (8.5)	This work
$HRu_3Rh(\eta^5\text{-Cp*})(CO)_9BH_2$		−9.6 (2H) [b]	−20.3	[6]
$HRu_3Rh(\eta^5\text{-Cp*})(CO)_8(PPh_3)BH_2$	Ru(wingtip)	−4.9	−14.4 (14); −20.6 [a]	[6]

[a] No ^{31}P–^{1}H coupling was resolved between the Ru(wingtip) phosphine and the Ru(hinge)–H–Ru(hinge) hydride.
[b] One broad signal assigned to both Rh–H–B and Ru–H–B.

useful set of data emphasizing a chemical shift correlation that can aid structural assignment. In the case of $HRu_3Rh(\eta^5\text{-}Cp^*)(CO)_9BH_2$, substitution of CO by PPh_3 occurs (in line with related systems) at the wingtip Ru atom, but is accompanied by the migration of the Rh–H–B cluster hydrogen atom to the metal framework. This is reflected, not only in the appearance of an additional metal hydride signal in the ^{1}H-NMR spectrum, but also in a much larger shift in the signal assigned to the Ru–H–B than is expected for a simple wingtip Ru substitution (Table 3).

4. Supplementary material

Crystallographic data for the structural analysis have been deposited with the Cambridge Crystallographic Data Centre, CCDC no. 140104. Copies of this information may be obtained free of charge from The Director, CCDC, 12 Union Road, Cambridge CB2 1EZ, UK (fax: +44-1223-336-033; e-mail: deposit@ccdc.cam.ac.uk or www: http://www.ccdc.cam.ac.uk).

Acknowledgements

We thank the EPSRC for a grant (to D.M.N.), the University of Basel, and the National Science Foundation for a grant (CHE 9007852) towards the purchase of a diffractometer at the University of Delaware.

References

[1] C.E. Housecroft, Chem. Soc. Rev. 24 (1995) 215.
[2] C.E. Housecroft, Coord. Chem. Rev. 143 (1995) 297.
[3] C.E. Housecroft, in: P. Braunstein, L. Oro, P.R. Raithby (Eds.), Metal Clusters in Chemistry, Wiley–VCH, Weinheim, 1999, p. 9.
[4] C.E. Housecroft, D.M. Matthews, A.L. Rheingold, X. Song, J. Chem. Soc. Dalton Trans. (1992) 2855.
[5] S.M. Draper, C.E. Housecroft, A.K. Keep, D.M. Matthews, X. Song, A.L. Rheingold, J. Organomet. Chem. 423 (1992) 241.
[6] J.R. Galsworthy, C.E. Housecroft, D.M. Matthews, R. Ostrander, A.L. Rheingold, J. Chem. Soc. Dalton Trans. (1994) 69.
[7] C.E. Housecroft, D.M. Nixon, A.L. Rheingold, Polyhedron 18 (1999) 2415.
[8] C.E. Housecroft, D.M. Matthews, A.J. Edwards, A.L. Rheingold, J. Chem. Soc. Dalton Trans. (1993) 2727.
[9] C.R. Eady, B.F.G. Johnson, J. Lewis, J. Chem. Soc. Dalton Trans. (1977) 477.
[10] F. Piacenti, M. Bianchi, P. Frediani, E. Benedetti, Inorg. Chem. 10 (1971) 2759.
[11] SHELXTL-PC software version 5: G. Sheldrick, Siemens XRD, Madison, WI.
[12] S.M. Draper, C.E. Housecroft, J.S. Humphrey, A.L. Rheingold, J. Chem. Soc. Dalton Trans. (1995) 3789.
[13] C.E. Housecroft, J.S. Humphrey, A.L. Rheingold, Inorg. Chim. Acta 259 (1997) 85.
[14] F.E. Hong, D.A. McCarthy, J.P. White, C.E. Cottrell, S.G. Shore, Inorg. Chem. 29 (1990) 2874.
[15] A.K. Chipperfield, C.E. Housecroft, A.L. Rheingold, Organometallics 9 (1990) 681.